Mid-Infrared Spectrum of the Gas-Phase Ethyl Peroxy Radical: C_2H_5OO

Daisy Ann Mah, Jose Cabrera, Humberto Nation, Mauricio Ramos, Shantanu Sharma, and Scott L. Nickolaisen*

Department of Chemistry & Biochemistry, California State University, 5151 State University Drive, Los Angeles, California 90032

Received: May 23, 2002; In Final Form: April 4, 2003

The mid-IR spectrum of gas-phase C_2H_5OO has been measured over the spectral range of 800−4000 cm^{-1}. The employed experimental technique was long-path-length absorption in which a White cell was coupled to an FTIR spectrometer. Radicals were generated in a mixing manifold prior to the absorption cell by passing an F_2/He mixture through a microwave discharge to create fluorine atoms followed by the reaction of atomic fluorine with an ethane/oxygen mixture. A number of absorption bands were observed to increase in intensity with increasing atomic fluorine concentration. Verification that the observed bands originated from the ethyl peroxy radical was done first by comparing measured band frequencies with the spectra of possible secondary reaction products and second by titrating $C_2H_5OO\bullet$ with excess nitric oxide and observing the nitrogen dioxide and ethyl nitrite products that ultimately result from the titration reaction. Bands were assigned to normal modes of $C_2H_5OO\bullet$ through comparing the observed band positions and intensities to the results of ab initio calculations and to the previous work of Chettur and Snelson (Chettur, G.; Snelson, A. *J. Phys. Chem.* **1987**, *91*, 3484) and Pushkarsky, Zalyubovsky, and Miller (Pushkarsky, M.B.; Zalyubovsky, S. J.; Miller, T. A. *J. Chem. Phys.* **2000**, *112*, 10695).

Introduction

Alkyl peroxy radicals ($RCH_2OO\bullet$) participate as essential intermediates in a variety of chemical systems including combustion and atmospheric chemistry. The oxidation of hydrocarbons to alkyl peroxy radicals is one of the most important reactions in combustion systems. Model simulations show that for hydrocarbon low-temperature flames the formation of the alkyl peroxy radical followed by isomerization to the hydroperoxy-alkyl radical is the dominant reaction pathway for the activation of hydrocarbons.[1] Our interest in alkyl peroxy radicals, however, stems from their importance in the formation of ozone in photochemical smog. In the troposphere, hydrocarbon oxidation is initiated by hydrogen atom abstraction by the hydroxyl radical followed by association with molecular oxygen to form the alkyl peroxy radical.[2] $RCH_2OO\bullet$ reacts with nitric oxide to create nitrogen dioxide and the alkoxy radical. Nitrogen dioxide undergoes photolysis to release an oxygen atom that subsequently combines with molecular oxygen to create ozone:

$$RCH_3 + \bullet OH \rightarrow RCH_2\bullet + H_2O$$

$$RCH_2\bullet + O_2 + M \rightarrow RCH_2OO\bullet + M$$

$$RCH_2OO\bullet + NO \rightarrow RCH_2O\bullet + NO_2$$

$$NO_2 + \text{sunlight} \rightarrow NO + O$$

$$O + O_2 + M \rightarrow O_3 + M$$

Alkoxy radicals subsequently react in one of three possible ways.[3] First, the alkoxy radical, $RCH_2O\bullet$, may react with molecular oxygen to form HO_2 and an aldehyde, RCHO. The aldehyde undergoes hydrogen abstraction by OH to form $RCO\bullet$, which may either dissociate to $R\bullet + CO$ or react with O_2 to form $RO\bullet + CO_2$. Both channels eventually result in the formation of an alkyl peroxy radical with one or more fewer carbon atoms. Second, $RCH_2O\bullet$ may decompose to form an alkyl radical and an aldehyde. The rate of decomposition depends on the identity of the departing alkyl group and increases for larger C_n. Thus, this channel becomes more important for $RCH_2O\bullet$ having three or more C atoms. The resulting alkyl radical associates with molecular oxygen to create a new alkyl peroxy radical with fewer carbon atoms, and the aldehyde will proceed with the reaction in the manner just described. Finally, $RCH_2O\bullet$ may isomerized by a 1,5 H-atom shift that proceeds through a six-membered ring that generates an alcohol functional group and an alkyl radical group separated by four carbon atoms. Of necessity, this occurs only for C_n ($n \geq 4$) alkoxy radicals. The radical product adds molecular oxygen to create an alkyl peroxy radical. The alkoxy + O_2 reaction dominates the loss mechanism for C_n ($n \leq 3$), and isomerization dominates for C_n ($n > 5$).[3]

Because of their essential participation in many chemical systems, it is important to have experimental techniques capable of monitoring alkyl peroxy radicals. Most studies of the reactions of alkyl peroxy radicals have employed UV absorption spectroscopy to monitor the strong $B^2A''-X^2A''$ transition centered at 240 nm that is common to all alkyl peroxy radicals. Although this method provides high sensitivity for peroxy radical detection, the broad nature of the UV absorption band results in spectral overlap with many other species that may be involved in peroxy radical chemistry. We therefore have embarked on a series of experiments to measure the infrared spectra of alkyl peroxy radicals in the gas phase so that IR techniques may be used to monitor various reactions of $ROO\bullet$ with the spectral

* To whom correspondence should be addressed. E-mail: snickol@calstatela.edu.

10.1021/jp026167r CCC: $25.00
Published on Web 05/10/2003

specificity inherent to the IR region. We have begun by measuring the IR spectrum of the ethyl peroxy radical, C_2H_5-OO•.

A variety of spectroscopic techniques[4−10] including UV absorption spectroscopy, flash photolysis/time-resolved UV spectroscopy, mass spectrometry, pulse radiolysis, and recently, near-IR cavity ring-down spectroscopy have been employed to elucidate the photokinetic and mechanistic information of ethyl peroxy radical reactions. IR bands of C_2H_5OO• have been reported in only two previous studies. Chettur and Snelson[11] pyrolyzed azoethane to form ethyl radical followed by deposition in a mixture of oxygen and argon at ∼10 K onto an optical substrate. Spectra of the resulting ethyl peroxy radical in an Ar matrix were recorded over the 200−4000 cm^{-1} range. Pusharsky et al.[12] monitored the $A^2A'-X^2A''$ transition of the ethyl peroxy radical in the region of 7600 cm^{-1} following the photolysis of either iodoethane or 3-pentanone in the presence of oxygen, and they observed an absorption band attributed to the O−O stretch of the gas-phase ethyl peroxy radical. This is the only known study that we could find in the literature to report frequencies of any vibrational band of the gas-phase ethyl peroxy radical. This paper reports the IR bands of C_2H_5OO• over the 800−4000 cm^{-1} region and the means by which we have verified the reported frequencies.

Experimental Section

The spectrum of the gas-phase ethyl peroxy radical was determined using a Fourier transform infrared spectrometer coupled to a long-path-length absorption cell. The IR output of a 0.1-cm^{-1} resolution FTIR spectrometer (Thermo Nicolet Nexus 870) was coupled to an absorption cell (Infrared Analysis model G-9-54X3-V-BA-AG). The absorption cell was equipped with White-type optics with a base absorption path of 2.74 m. The total absorption path length could be varied up to 150 m, although spectra reported in this paper were typically collected with a 90-m optical path. The absorption cell was fitted with BaF_2 windows. A HgCdTe detector with a 1-mm^2 active area (Cincinnati Electronic, model MDD-10E0-S) was mounted at the exit of the absorption cell, and the detector signal was returned to the FTIR for processing via a BNC cable. Spectra were recorded at a resolution of 1.0 cm^{-1}. Interferogram scans (5000) were also typically added to produce the final recorded spectrum. The choice of detector and window material limited the useful spectral range of the apparatus to the region of 800−4000 cm^{-1}. The transfer optics between the spectrometer, absorption cell, and detector were enclosed within an acrylic box that was continually purged with dry, CO_2-free air to eliminate background signals from atmospheric water and carbon dioxide.

The ethyl peroxy radical was generated by the reaction mechanism

$$F_2 + \mu\text{wave} \rightarrow 2F$$

$$F + C_2H_6 \rightarrow \bullet C_2H_5 + HF$$

$$\bullet C_2H_5 + O_2 \rightarrow C_2H_5OO\bullet$$

Ethyl peroxy radicals were created in a 3.8-cm-diameter × 70-cm-length mixing manifold that was connected to the absorption cell with 0.5-in. o.d. stainless tubing. Atomic fluorine was formed by flowing a mixture of 5% F_2 in UHP helium through a microwave cavity connected to an rf generator. The microwave cavity encased a 0.5-in. o.d. alumina ceramic tube in which the discharge was maintained. Ethane was added to the gas flow beyond the discharge but prior to the mixing manifold. Ethane was allowed to react with F atoms by flowing through ∼0.7 m of 0.25-in. o.d. Teflon tubing before entering the mixing manifold. UHP oxygen was added directly within the mixing manifold. Flows of all gases were measured with calibrated mass flow meters. The total pressure within the mixing manifold was monitored with a 100-Torr capacitance manometer and typically ranged from 1.5 to 3.0 Torr. A schematic of the experimental apparatus is shown in Figure 1.

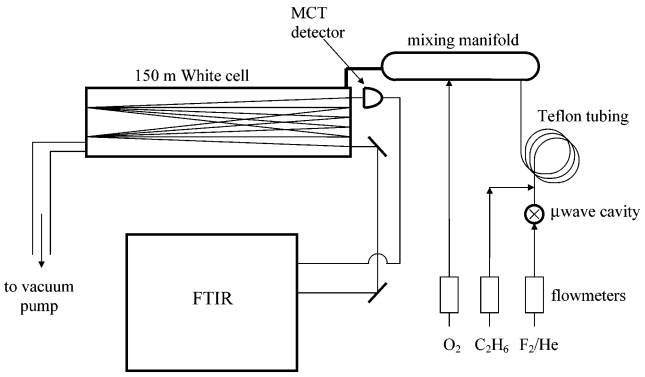

Figure 1. Schematic of the FTIR/long-path-length absorption apparatus.

It was necessary to record two spectra to observe the vibrational bands of the ethyl peroxy radical. The first spectrum was collected with all gases flowing at the desired concentrations but with the microwave discharge off. The observed spectrum under these conditions was that of ethane because no other gases in the system exhibit absorption in the IR region. The flow rate of ethane was adjusted such that the absorbance of the CH_3 deformation modes in the region of 1300−1500 cm^{-1} had a maximum value of $A < 1$. At these concentrations, the stronger bands of ethane in the C−H stretching region around 3000 cm^{-1} were in the nonlinear regime of Beer's law with $A \gg 1$. A second spectrum was then recorded using the same gas-flow rates with the microwave discharge turned on. This spectrum included bands not only from ethane but also from the ethyl peroxy radical and other reaction products formed by secondary chemistry. The peroxy radical spectrum was obtained by subtracting the discharge-off spectrum from the discharge-on spectrum. Subtractions were optimized to produce a smooth baseline over the CH_3 deformation region. It was difficult to achieve a smooth baseline in the C−H stretching region because the large signals due to C_2H_6 were in the nonlinear regime of Beer's law and small variations in ethane concentrations over the duration of an acquisition could not be evenly subtracted out.

The spectrum of the ethyl peroxy radical was confirmed by performing titration experiments with nitric oxide. The reaction $C_2H_5OO\bullet + NO \rightarrow C_2H_5O\bullet + NO_2$ has a room-temperature rate coefficient of $k_{298} = 9 \times 10^{-12}$ cm^3 $molecule^{-1}$ s^{-1}.[18] For these measurements, excess nitric oxide was first passed through a glass cartridge containing Ascarite II to remove any NO_2 impurity. NO was then added to the flow of gas from the mixing manifold through a T joint in the 0.5-in. o.d. tubing connecting the mixing manifold to the absorption cell.

Ab initio calculations of the C_2H_5OO• ground electronic state were used to assist in the assignment of normal-mode frequencies. Calculations were performed with the Gaussian 98 software suite running on 1.0-GHz Pentium 4 processor. Geometries were optimized and energies were determined using B3LYP density functional theory with a 6-311G basis set. Frequencies, normal-mode motions, and transition intensities were calculated at the

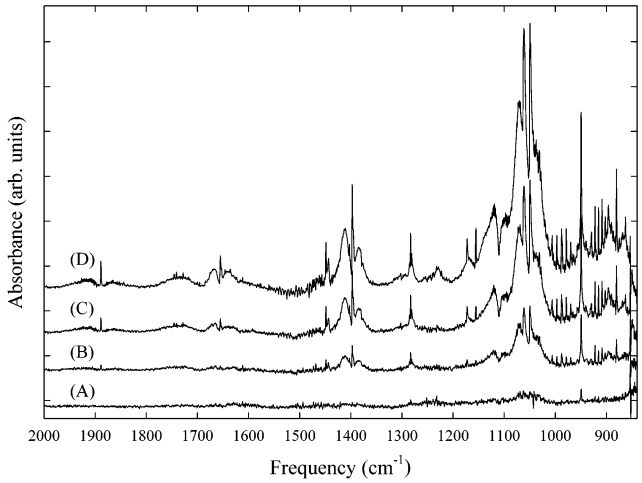

Figure 2. Spectra resulting when a mixture of C_2H_6, O_2, and F atoms in He is combined in a mixing manifold at flow rates of 40 sccm C_2H_6, 400 sccm O_2, and (A) 10 sccm F_2/He, (B) 30 sccm F_2/He, (C) 60 sccm F_2/He, and (D) 100 sccm F_2/He. The total pressure is 1.5 Torr.

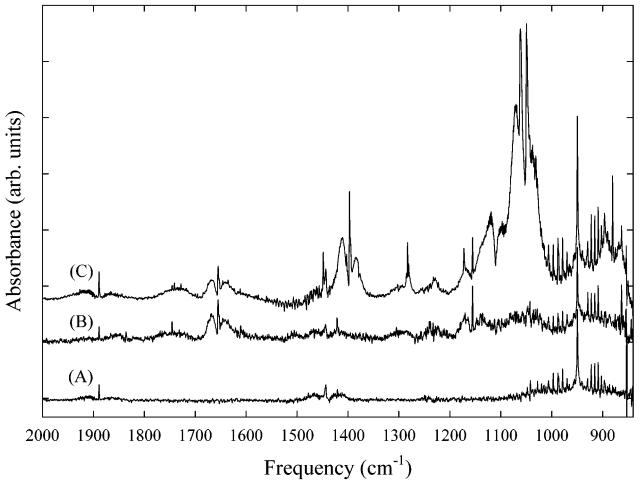

Figure 3. Comparison of the spectra of (A) pure C_2H_4, (B) C_2H_4 with F atoms and O_2 added, and (C) trace D of Figure 2.

same level of theory using the optimized geometries. Harmonic frequencies were scaled by a factor of 0.9613 to account for the anharmonicity of the potential surface.

Results and Discussion

A series of spectra recorded with constant concentrations of ethane and oxygen and as a function of increasing fluorine concentration are shown in Figure 2. The concentrations of ethane and oxygen were constant at values of $[C_2H_6] = 3.0 \times 10^{15}$ molecule cm^{-3} and $[O_2] = 4.3 \times 10^{16}$ molecule cm^{-3}. The concentration of F_2 flowing through the microwave discharge was varied from 5.4×10^{13} to 6.0×10^{14} molecule cm^{-3}. A number of bands were observed to increase in intensity with increasing atomic fluorine concentration, as seen in Figure 2. To assign the observed bands to the ethyl peroxy radical, it is first necessary to consider all of the possible secondary chemical reactions that may occur in the system and identify any bands that may originate from intermediate or stable species resulting from secondary reactions.

When the flow of ethane into the mixing manifold was turned off and only oxygen and fluorine were in the mixing manifold, none of the bands observed in Figure 1 were present, indicating that all of these bands originate from the initiation reaction of $F + C_2H_6$. When the flow of oxygen was turned off and only ethane and fluorine were present in the system, only the band centered at 950 cm^{-1}, displaying a distinct Q branch and rotationally resolved P and R branches, was seen. This band was assigned to ethylene, C_2H_4. Ethylene can be formed in this reaction system in the presence of excess atomic fluorine by the mechanism

$$F + C_2H_6 \rightarrow \bullet C_2H_5 + HF$$

$$F + \bullet C_2H_5 \rightarrow C_2H_4 + HF$$

Thus, in the absence of oxygen, the ethylene spectrum is observed, but it is also observed with all gases present in the mixing manifold, indicating that the ethyl radical formed following the hydrogen abstraction undergoes competitive reaction with either molecular oxygen to form the ethyl peroxy radical or with atomic fluorine to form ethylene.

To identify bands that might arise from the secondary chemistry of ethylene, a series of measurements were performed in which ethane was replaced by ethylene in the mixing manifold. The results are shown in Figure 3. Trace A shows the spectrum of a mixture of ethylene and oxygen in the absence of atomic fluorine. As expected, the spectrum is that of ethylene with the rotationally resolved band at 949 cm^{-1} and a weaker band at 1443 cm^{-1} that is not completely resolved at the resolution of our instrument. Trace B is the spectrum resulting when atomic fluorine is added to the mixing manifold with ethylene and oxygen. Under these conditions, three additional bands appear at 863, 1155, and 1655 cm^{-1}. Trace C in Figure 2 is the same as trace D in Figure 1 and is included to facilitate comparison between the two sets of measurements.

Ethylene may undergo reaction with atomic fluorine through one of three possible product channels:

$$F + C_2H_4 \rightarrow CH_2CH_2F \qquad k_{298} = 5.1 \times 10^{-12}\ \text{cm}^3\ \text{molecule}^{-1}\ \text{s}^{-1}\ ^{13} \quad (1a)$$

$$\rightarrow CH_2CHF + H \qquad k_{298} = 2.3 \times 10^{-11}\ \text{cm}^3\ \text{molecule}^{-1}\ \text{s}^{-1}\ ^{14} \quad (1b)$$

$$\rightarrow C_2H_3 + HF \qquad k_{298} = 3.5 \times 10^{-11}\ \text{cm}^3\ \text{molecule}^{-1}\ \text{s}^{-1}\ ^{15} \quad (1c)$$

Reaction 1a is slow relative to the other two channels and is assumed not to participate significantly in the formation of secondary chemical products. An examination of the spectra in Figures 2 and 3 indicates that the bands occurring under both sets of experimental conditions at 863, 1155, and 1655 cm^{-1} originate from fluoroethylene (CH_2CHF). The vinyl radical formed in reaction 1c will undergo further reaction by association with molecular oxygen to create the vinyl peroxy radical:

$$C_2H_3 + O_2 \rightarrow C_2H_3OO\bullet \qquad k_{298} = 1.0 \times 10^{-11}\ \text{cm}^3\ \text{molecule}^{-1}\ \text{s}^{-1}\ ^{16} \quad (2)$$

There are two other possible product channels for this reaction to form either $CH_2CHO + O$ or $C_2H_2 + HO_2$, but room-temperature rate coefficients for these reactions, calculated using RRKM theory, are at least 2 orders of magnitude slower than those of reaction 1.[17] However, all of the bands observed in trace B of Figure 3 may be assigned to either ethylene or fluoroethylene; we see no experimental evidence for the formation of the vinyl peroxy radical through reactions 1c and 2.

TABLE 1: Comparison of Observed Gas-Phase Ethyl Peroxy Radical Band Frequencies with ab Initio Calculations, Ar Matrix Data, and Known Bands of Other Possible Secondary Chemistry Products[a]

C_2H_5OO assignment	this work	ab initio (rel inten)	Ar matrix[11]	C_2H_5O assignment[28]		CH_3CHO assignment[29]		CH_3OH assignment[29]	
ν_1 CH_3 in-plane str	2988 m	2986 (0.60)				CH_3 assym str	3005 m	O−H str	3681 m
ν_2 CH_3 out-plane str		2987 (0.02)				CH_3 assym str	2967 m	CH_3 assym str	3000 m
ν_3 CH_3 sym. str		2918 (0.35)				CH_3 sym str		CH_3 assym str	2960 s
ν_4 CH_2 assym str	2999 s	3013 (1.0)	3016 w			C−H str	2822 m	CH_3 sym str	2844 s
ν_5 CH_2 sym str	2964 s	2945 (0.28)							
ν_6 CH_3 in-plane def	1448 m	1485 (0.24)	1451 s			CH_3 assym def	1441 s	CH_3 assym def	1477 m
ν_7 CH_3 out-of-plane def	1397 s	1464 (0.25)	1389 vs			CH_3 assym def	1420 s		
ν_8 CH_3 sym def		1403 (0.39)	1380 s			CH_3 sym def	1352 s	CH_3 sym def	1455 m
ν_9 CH_3 out-of-plane rock		1242 (0.00)				CH_3 rock	919 m	CH_3 rock	1165
ν_{10} CH_3 in-plane rock	1110 m	1104 (0.15)	1136 m			CH_3 rock	867 m	CH_3 rock	1060 w
ν_{11} CH_2 scissor		1473 (0.07)	1474 m	CH_2 scissor	1295				
ν_{12} CH_2 wag	1283 m	1341 (0.46)	1351 m	CH_2 wag	1370	C−H bend	1400 s	O−H bend	1345 s
ν_{13} CH_2 twist	1173 w	1115 (0.17)	1242 w						
ν_{14} CH_2 rock		795 (0.04)	800 m			C−H bend	763 w		
ν_{15} O−O str	1050, 1062, 1070 vs	1020 (0.44)	1112 m						
ν_{16} C−C str	880 s	982 (0.42)	1009 s	C−C str	875	C−C str	1113 s		
ν_{17} C−O str		773 (0.17)	838 m	C−O str	1067	C−O str	1743 vs	C−O str	1033 vs
ν_{18} COO bend		462 (0.23)	499 vs	CCO bend	442	CCO bend	509 s		
ν_{19} CO torsion		66 (0.00)				torsion	150 w	torsion	295
ν_{20} CC torsion		207 (0.01)							
ν_{21} CCO bend		285 (0.04)							

[a] Frequencies are given in cm^{-1}. Relative intensities for ab initio bands are given in parentheses.

There are additional secondary reactions involving the ethyl peroxy radical that must also be considered. If excess fluorine atoms are present, then they will react with the ethyl peroxy radical by abstracting either an oxygen atom or a hydrogen atom. The mechanisms are

$$C_2H_5OO\bullet + F \rightarrow C_2H_5O\bullet + FO \quad (3a)$$

$$C_2H_5O\bullet + O_2 \rightarrow CH_3CHO + HO_2$$
$$k_{298} = 1.0 \times 10^{-14}\ cm^3\ molecule^{-1}\ s^{-1}\ ^{18} \quad (3b)$$

$$C_2H_5OO\bullet + F \rightarrow \bullet C_2H_4OO\bullet + HF$$
Criegee biradical formation (3c)

$$\bullet C_2H_4OO\bullet \rightarrow CH_4 + CO_2 \quad (3d)$$

$$\rightarrow CH_3OH + CO \quad (3e)$$

Because oxygen is the major component of the gas mixture with a concentration of $[O_2] = 4.3 \times 10^{16}$ molecule cm^{-3}, the lifetime of the ethoxy radical in reaction 3b is approximately 2.5 ms, which is much shorter than the residence time of the gases within the cell, so the conversion of the ethoxy radical to acetaldehyde should be essentially complete on the measurement time scale in this system.

Rate coefficients for the decomposition reactions of the ethyl Criegee biradical have not been reported previously. The analogous biradical, $\bullet CH_2OO\bullet$, stemming from the methyl peroxy radical has a decomposition rate of $6.0 \times 10^4\ s^{-1}$ for the $H_2O + CO$ channel.[19] On the basis of this comparison and the instability of the biradical, the decomposition of $\bullet C_2H_4OO\bullet$ is expected to be very fast.

The resulting stable end-products from the possible secondary chemistry originating from reactions of the ethyl peroxy radical are acetaldehyde, methane, methanol, carbon monoxide, and carbon dioxide. A close examination of the spectra of Figure 2 reveals no evidence of CO or CO_2 absorptions in the appropriate spectral regions. Table 1 compares the frequencies and intensities of the other possible stable end-products mentioned above with those bands observed in this study that cannot be attributed to the chemistry of ethylene. It is clear that many of the bands observed when ethane is present in the manifold cannot be attributed to acetaldehyde, methane, or methanol.

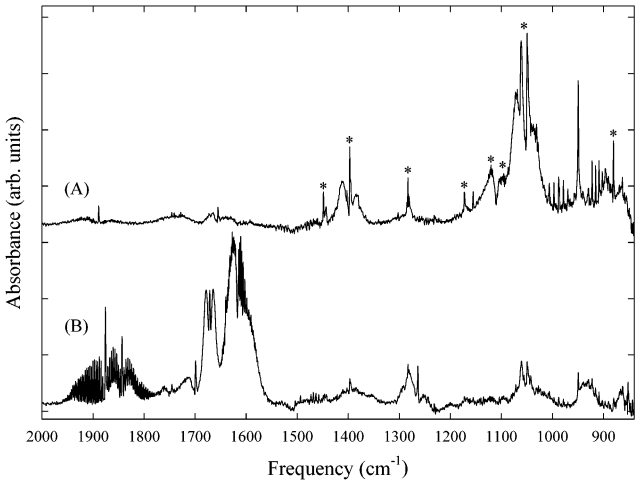

Figure 4. Spectrum resulting from the addition of excess NO to C_2H_5-OO. (A) Titration spectrum with excess NO. (B) Spectrum from trace C of Figure 2 for comparison. (∗) Bands attributed to C_2H_5OO.

To further verify that the spectrum recorded in Figure 2 stems from the ethyl peroxy radical, a set of titration experiments were performed in which nitric oxide was added to the gas flow from the mixing manifold just prior to the absorption cell. The reaction between the ethyl peroxy radical and nitric oxide to form the ethoxy radical and nitrogen dioxide is reasonably fast, so it is expected that the titration will be complete:

$$C_2H_5OO\bullet + NO \rightarrow C_2H_5O\bullet + NO_2$$
$$k_{298} = 8.7 \times 10^{-12}\ cm^3\ molecule^{-1}\ s^{-1}\ ^{20}$$

The results of the titration measurements are shown in Figure 4. Trace B is the spectrum recorded with the addition of excess NO. Trace A of Figure 3 is the same spectrum as that shown in Figure 2, trace C and is included in the Figure to facilitate comparison. It is clear that the spectrum measured with excess NO is very different from that seen without nitric oxide. The challenge is to identify all of the bands seen in Figure 4B and

correlate them with the chemistry of the system under these conditions. The rotationally resolved band centered at 1876 cm^{-1} is that of NO, and the strong band observed at 1617 cm^{-1} stems from NO_2. The NO_2 seen in this measurement does not come from contamination in the nitric oxide gas cylinder because NO is passed through an Ascarite trap prior to its addition to the cell, and spectra recorded with the microwave discharge off show no evidence of NO_2. The source of the NO_2 is the titration reaction. There is also another rotationally resolved band at 1843 cm^{-1} that is assigned to nitrosyl fluoride, FNO. FNO may be formed either by the association reaction between NO and atomic fluorine with a third-order rate coefficient of $k_{298} = 1.8 \times 10^{-31}$ cm^6 $molecule^{-2}$ s^{-1} [18] or by the bimolecular reaction of molecular fluorine and NO with a rate coeffcient of $k_{298} = 1.5 \times 10^{-14}$ cm^3 $molecule^{-1}$ s^{-1}.[19] Both reactions contribute approximately equally under the experimental conditions of this study.

The $C_2H_5O\bullet$ product of the titration reaction will undergo further reaction within the mixing manifold. Specifically, the ethoxy radical may react with either NO directly or the NO_2 product formed in the titration reaction:

$$C_2H_5O\bullet + NO \rightarrow CH_3CHO + HNO \qquad k_{298} = 1.3 \times 10^{-11}\ cm^3\ molecule^{-1}\ s^{-1}$$ [22]

$$\xrightarrow{M} C_2H_5ONO \qquad k_{298} = 5.0 \times 10^{-11}\ cm^3\ molecule^{-1}\ s^{-1}$$ [18,21b]

$$C_2H_5O\bullet + NO_2 \rightarrow CH_3CHO + HNO_2 \qquad k_{298} = 6.6 \times 10^{-12}\ cm^3\ molecule^{-1}\ s^{-1}$$ [22]

$$\xrightarrow{M} C_2H_5ONO_2 \qquad k_{298} = 2.8 \times 10^{-11}\ cm^3\ molecule^{-1}\ s^{-1}$$ [18]

Under our experimental conditions with total pressure in the range of 1.0−2.0 Torr, the reactions of the ethoxy radical with both NO and NO_2 are in the high-pressure limit, so the bimolecular rate coefficients of the association reactions are the appropriate values to use in assessing possible secondary reactions. Comparing the titration spectrum with the reported spectrum of ethyl nitrite[23] (C_2H_5ONO) confirms that the bands at 935, 1050, 1395, and 1672 cm^{-1} arise from this species. The bands at 863 and 1281 cm^{-1} are in good agreement with the reported frequencies of gas-phase ethyl nitrate ($C_2H_5ONO_2$).[30] There is no spectral evidence for CH_3CHO, HNO, or HNO_2 in trace A of Figure 4.

The bands marked by asterisks in trace B of Figure 4 are those originating from the ethyl peroxy radical in the range of 850−2000 cm^{-1}. These assignments are based on considerations of the behavior of the bands with increasing fluorine added to the mixing manifold, the secondary chemistry expected to occur in the reaction system, and the titration of the ethyl peroxy radical with excess nitric oxide. The results are summarized in Table 1. Included in Table 1 are tentative assignments of the bands to specific vibrational modes.

A series of measurements were also performed to examine the ethyl peroxy radical bands in the C−H stretching region around 3000 cm^{-1} carefully. The spectra shown in Figure 2 result from subtracting the discharge-off data from the discharge-on data. The largest band in the ethane spectrum is at 3000 cm^{-1}, and at the C_2H_6 concentrations used for the spectra of Figure 2, the absorbance of this band is in the nonlinear range of Beer's law, so simple subtraction does not result in the clean

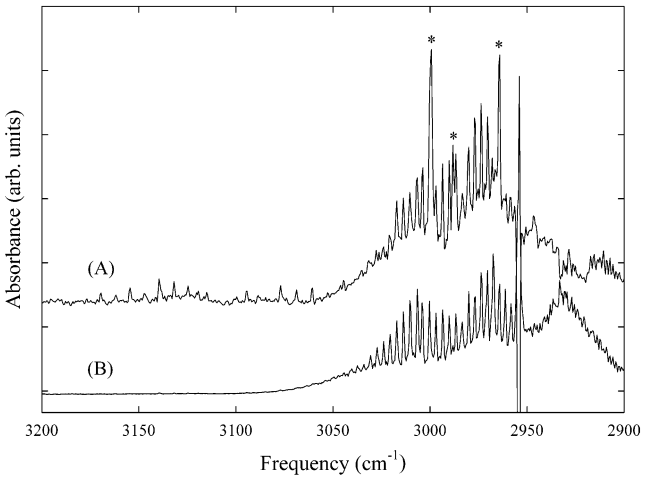

Figure 5. Spectrum of C_2H_5OO in the C−H stretching region from 2900 to 3200 cm^{-1}. (A) Spectrum of C_2H_5OO. (B) Spectrum of pure ethane for comparison. (∗) Bands attributed to C_2H_5O.

removal of bands arising from parent ethane throughout this spectral region. Thus, it was necessary to decrease the amount of ethane in the mixing manifold by a factor of ∼2.5 to reduce the absorbance of the bands to less than 1. However, the consequence of this decrease in $[C_2H_6]$ is weaker signals from the peroxy radical. The resulting spectrum over the 2900−3200 cm^{-1} range is shown in trace A of Figure 5. The weak P and R branches centered about 3105 cm^{-1} are from C_2H_4. The mechanism for ethylene formation is discussed above. Trace B is a spectrum of ethane scaled so that the rotational bands are approximately the same size as those seen in trace A. Even following the best possible subtraction of the ethane spectrum from the ethyl peroxy radical spectrum, there are still rotational lines observed in trace A. A very careful comparison of the two spectra reveals that some of these rotationally resolved lines in the two traces are at slightly different positions. However, the resolution of these measurements is not sufficient to assign unique line positions. There are, however, three lines in trace A that are distinctly different from those of pure ethane, and these have been marked with asterisks. Additionally, the three labeled lines disappear upon the addition of excess nitric oxide in the titration measurements. On the basis of the above considerations, we assign these bands to the stretching modes of the ethyl peroxy radical. The band positions are included in Table 1.

The vibrational-mode assignments listed in Table 1 for the gas-phase frequencies of the ethyl peroxy radical were made with assistance from frequencies and band intensities computed by B3LYP density functional theory calculations using a 6-311G basis set and based on comparison to the two previous experimental studies. Agreement between calculated and experimental frequencies is less than 5% for all bands except the C−C stretching mode.

The most complete experimental work on ethyl peroxy radical spectroscopy is that of Chettur and Snelson.[11] They observed a number of bands ascribed to $C_2H_5OO\bullet$ in Ar matrix data. Their mode assignments were based on the frequency shifts measured when using isotopically labeled $^{18}O_2$ versus $^{16}O_2$ in the deposition step coupled with comparisons to calculated frequencies from a private communication of A. Wagner and C. Melius. In general, the Ar matrix frequencies are greater than gas-phase frequencies by an average deviation of 44 cm^{-1}. This is larger than expected when compared to other radical species for which both gas-phase and matrix frequencies have been reported.

We have estimated the maximum uncertainty of the Chettur and Snelson assignments to be on the order of 20 cm^{-1}. Because there are no other published studies of the mid-IR spectrum of the ethyl peroxy radical in an Ar matrix with which to compare the Chettur and Snelson measurements, our uncertainty assessment is based on an analysis of methyl peroxy radical spectra reported by the Snelson group and by Nandi et al.[24,25] Both studies measured the mid-IR spectrum of CH_3O_2 in an Ar matrix at ~12 K. Both groups generated the methyl radical by the pyrolysis of either methyl iodide or azomethane: Ase et al. co-deposited the methyl radical and oxygen on the cold substrate, and Nandi et al. did this in a hyperthermal nozzle apparatus in which the deposition of the methyl radical and oxygen on the cold substrate was alternated. Each group reported IR bands for the isotopic species CH_3O_2, $^{13}CH_3O_2$, $CH_3{}^{18}O_2$, and CD_3O_2. Thirty-two bands were assigned in common between the two studies. In general, the frequencies reported by Ase et al. were higher than those reported by Nandi et al. The deviations in assigned frequencies for specific bands ranged from 0 cm^{-1} up to a maximum of 170 cm^{-1}. The average deviation between assigned band centers was 22.5 cm^{-1} with a standard deviation of 58.2 cm^{-1}. We observed the same trend in comparing the gas-phase ethyl peroxy radical frequencies with the Ar matrix frequencies reported by Chettur and Snelson.

In addition, Pusharsky et al. used cavity ring-down spectroscopy to observe the $A^2A'-X^2A''$ transition of $C_2H_5OO\bullet$.[12] They measured a band centered at 7590 cm^{-1} that was assigned to the O−O stretching mode of the gas-phase ethyl peroxy radical. It is expected that this low-lying electronic transition borrows oscillator strength from the molecular motion of the fundamental vibrational modes in much the same manner that the low-lying electronic transition in HO_2 does.[26,27] As a result, the spectral features and overall shape of the observed $C_2H_5OO\bullet$ electronic transition at 1.32 μm should be similar to that of the rovibrational band observed in the mid-IR region. A comparison of the spectrum reported by Pusharsky et al. with the band centered at 1055 cm^{-1} confirms the similarity, so we assign this band to the O−O stretching mode of $C_2H_5OO\bullet$. This provides additional confidence that the bands reported in this work originate from the gas-phase ethyl peroxy radical.

Conclusions

We have measured the IR spectrum of the ethyl peroxy radical in the gas phase over the range of 800−4000 cm^{-1}. The bands ascribed to $C_2H_5OO\bullet$ behaved properly when excess nitric oxide was included in the mixing manifold in that these bands all decreased in intensity with the addition of NO. Comparison to the previously reported IR studies of $C_2H_5OO\bullet$ provided further verification of the spectrum and assisted in assigning the bands to vibrational normal modes. The results presented here will be used to study the kinetics of the ethyl peroxy radical with a number of reaction partners using time-resolved infrared techniques.

Acknowledgment. This work was support by funding from the NIH MBRS program, grant number S06 GM 8101-30 and by funding from the NASA Faculty Award for Research program, contract number 1210167. Portions of the support for J.C., H.N., and M.R. were provided by the NSF Research Experience for Undergraduates program, grant number CHE-9731839. We also acknowledge support from the CSULA College of Natural and Social Sciences.

References and Notes

(1) Curran, H. J.; Gaffuri, P.; Pitz, W. J.; Westbrook, C. K. *Combust. Flame* **1998**, *114*, 149.

(2) Lightfoot, P. D.; Cox, R. A.; Crowley, J. N.; Destriau, M.; Hayman, G. D.; Jenkin, M. E.; Moortgat, G. K.; Zabel, F. *Atmos. Environ., Part A* **1992**, *26*, 1805.

(3) Atkinson, R. *Int. J. Chem. Kinet.* **1997**, *29*, 99.

(4) Hunziker, H. E.; Wendt, H. R. *J. Chem. Phys.* **1976**, *64*, 3446.

(5) Adachi, H.; Basco, N.; James, D. G. L. *Int. J. Chem. Kinet.* **1979**, *11*, 1211.

(6) Maricq, M. M.; Szente, J. J. *J. Phys. Chem.* **1994**, *98*, 2078.

(7) Ellerman, T. J.; Maricq, M. M. *J. Phys. Chem.* **1992**, *96*, 982.

(8) Plumb, I. C.; Ryan, K. R. *Int. J. Chem. Kinet.* **1981**, *13*, 1011.

(9) Munk, J.; Pagsberg, P.; Ratajczak, E.; Sillesen, A. *J. Phys. Chem.* **1986**, *90*, 2752.

(10) Atkinson, D. B.; Hudgens, J. W. *J. Phys. Chem. A* **1997**, *101*, 3901.

(11) Chettur, G.; Snelson, A. *J. Phys. Chem.* **1987**, *91*, 3483.

(12) Pushkarsky, M. B.; Zalyubovsky, S. J.; Miller, T. A. *J. Chem. Phys.* **2000**, *112*, 10695.

(13) Milstein, R.; Williams, R. L.; Rowland, F. S. *J. Phys. Chem*. **1974**, *78*, 857.

(14) Slagle, I. R.; Gutman, D. *J. Phys. Chem*. **1983**, *87*, 1818.

(15) Smith, D. J.; Setser, D. W.; Kim, K. C.; Bogan, D. J. *J. Phys. Chem*. **1977**, *81*, 898.

(16) Bozzelli, J. W.; Dean, A. M. *J. Phys. Chem*. **1993**, *97*, 4427.

(17) Mebel, A.m.; Diau, E. W. G.; Lin, M. C.; Morokuma, K. *J. Am. Chem. Soc*. **1996**, *118*, 9759.

(18) DeMore, W. B.; Sander, S. P.; Golden, D. M.; Hampson, R. F.; Kurylo, M. J.; Howard, C. J.; Ravishankara, A. R.; Kolb, C. E.; Molina, M. J. *Chemical Kinetics and Photochemical Data for Use in Stratospheric Modeling*, evaluation number 12; JPL Publication 97-4, 1997.

(19) Baulch, D. L.; Duxbury, J.; Grant, S. J.; Montague, D. C. *J. Phys. Chem. Ref. Data* **1981**, *4* (Supplement), 10.

(20) Maricq, M. M.; Szente, J. J.; Kaiser, E. W.; Shi, J. *J. Phys. Chem*. **1994**, *98*, 2083.

(21) (a) Maricq, M. M.; Szente, J. J. *J. Phys. Chem*. **1996**, *100*, 12374. (b) Daele, V.; Ray, A.; Vassalli, I.; Poulet, G.; Le Bras, G. *Int. J. Chem. Kinet*. **1995**, *27*, 1121. (c) Wallington, T. J.; Dagaut, P.; Kurylo, M. J. *Chem. Rev*. **1992**, *92*, 667. (d) Plumb, I. C.; Ryan, K. R.; Steven, J. R.; Mulcahy, M. F. R. *Int. J. Chem. Kinet*. **1982**, *14*, 183. (e) Adachi, H.; Basco, N. *Chem. Phys. Lett*. **1979**, *64*, 431.

(22) (a) Batt, L.; Milne, R. T. *Int. J. Chem. Kinet*. **1977**, *9*, 549. (b) Arden, E. A.; Phillips, L.; Shaw, R. *J. Chem. Soc*. **1964**.

(23) Klaboe, P.; Jones, D.; Lippincott, E. R. *Spectrochim. Acta, Part A* **1967**, *23*, 2957.

(24) Ase, P.; Bock, W.; Snelson, A. *J. Phys. Chem*. **1986**, *90*, 2099.

(25) Nandi, S.; Blanksby, S. J.; Zhang, X.; Nimlos, M. R.; Dayton, D. C.; Ellison, G. B. *J. Phys. Chem. A* **2002**, *106*, 7547.

(26) Tuckett, R. P.; Freedman, P. A.; Jones, W. J. *Mol. Phys.* **1979**, *37*, 379.

(27) Osmann, G.; Bunker, P. R.; Jensen, P.; Buenker, R. J.; Gu, J.; Hirsch, G. L. *Mol. Spectrosc*. **1999**, *197*, 262.

(28) (a) Inoue, G.; Okuda, M.; Akimoto, H. *J. Chem. Phys*. **1981**, *75*, 2060. (b) Ramond, T. M.; Davico, G. E.; Schwartz, R. L.; Lineberger, W. C. *J. Chem. Phys.* **2000**, *112*, 1158.

(29) Shimanouchi, T. *Tables of Molecular Vibrational Frequencies;* National Bureau of Standards: Washington, DC, 1972; Vol. 1, pp 1−160.

(30) Beresneva, G. A.; Khristenko, L. V.; Pentin, V. A. *Vestn. Mosk. Univ., Ser. 2: Khim.* **1985**, *26(1)*, 34.